

OPTIMIZATION OF OPERATIONAL CONDITIONS FOR SCANDIUM DETERMINATION IN ALUMINUM ALLOYS BY INDUCTIVELY COUPLED PLASMA OPTICAL EMISSION SPECTROMETRY

G. Ningxin

Research Institute of Physical and Chemical Engineering of Nuclear Industry,
Tianjin 300180, China; e-mail: ningxin_bit@hotmail.com

A method for the determination of scandium (Sc) in aluminum alloy samples by inductively coupled plasma optical emission spectrometry was developed. The method was optimized by the Box–Behnken design, which evaluated the operational conditions (radio frequency power, nebulizer gas flow rate, and sample flow rate). The optimum conditions were established as a radio frequency power of 1300 W, a nebulizer gas flow rate of 0.83 L/min, and a sample flow rate of 0.9 mL/min. Satisfactory performance characteristics (background equivalent concentration, limits of detection and quantification) were obtained under the optimum conditions. The method proposed using the optimum conditions allowed Sc determination with limits of detection and quantification of 0.15 and 0.48 $\mu\text{g/L}$, respectively. The accuracy of the proposed method was confirmed by analyzing an aluminum alloy certified reference material and performing a standard addition method. The standard addition experiments resulted in recoveries between 96.5% and 105%. The method developed has been applied to the Sc determination in aluminum alloy samples from the Beijing Institute of Aeronautical Materials, and the recovery study results ranged between 98.0 and 100.5%.

Keywords: scandium, aluminum alloy, operational conditions, inductively coupled plasma optical emission spectrometry.

ОПТИМИЗАЦИЯ РАБОЧИХ УСЛОВИЙ ПРИ ОПРЕДЕЛЕНИИ СКАНДИЯ В АЛЮМИНИЕВЫХ СПЛАВАХ МЕТОДОМ ОПТИЧЕСКОЙ ЭМИССИОННОЙ СПЕКТРОМЕТРИИ С ИНДУКТИВНО-СВЯЗАННОЙ ПЛАЗМОЙ

G. Ningxin

УДК 543.423

Научно-исследовательский институт физико-химической инженерии
атомной промышленности, Тяньцзинь, 300180, Кунтай; e-mail: ningxin_bit@hotmail.com

(Поступила 21 января 2019)

Разработан метод определения скандия (Sc) в образцах алюминиевого сплава с помощью оптической эмиссионной спектрометрии с индуктивно-связанной плазмой. Метод оптимизирован с помощью конструкции Бокса–Бенкена, в которой оценивались рабочие условия (мощность ВЧ-сигнала, расход газа распылителя и расход пробы). Определены оптимальные условия, в том числе мощность ВЧ-сигнала 1300 Вт, расход газа распылителя 0.83 л/мин и расход пробы 0.9 мл/мин. При этих условиях получены удовлетворительные рабочие характеристики, включающие в себя фоновую эквивалентную концентрацию, пределы обнаружения и количественного определения. В результате оптимизации метод позволяет определить содержание Sc с пределами обнаружения и количественного определения 0.15 и 0.48 мкг/л, его точность подтверждена путем анализа сертифицированного эталонного материала из алюминиевого сплава и использования метода стандартных добавок. Эксперименты со стандартными добавками приводят к восстановлению в пределах 96.5–105.0%. Разработанный метод применен для определения Sc в образцах алюминиевых сплавов Пекинского института авиационных материалов. Полученные данные восстановления находятся в интервале 98.0–100.5%.

Ключевые слова: скандий, алюминиевый сплав, рабочие условия, индуктивно-связанная плазма, оптическая эмиссионная спектрометрия.

Introduction. Aluminum alloys are widely used in the aerospace field due to their high specific strength, excellent electrical and thermal conductivity, and corrosion resistance [1, 2]. The ever-increasing demands for lightweight alloys with improved mechanical and corrosion resistance performances in the aerospace and aeronautic industries have led to the development of novel materials and advanced processing techniques. Therefore, improving the mechanical properties and corrosion resistance of aerospace aluminum alloys has been a subject of interest. Currently, the addition of rare-earth elements into aluminum alloys has been demonstrated to be an effective approach to improve their microstructure and mechanical properties [3, 4]. As one of the most efficient trace elements to improve the mechanical properties of alloys, scandium (Sc) has attracted much attention for aluminum alloys in recent years [5]. It has been reported that Sc acts as a grain refiner and recrystallization inhibitor [6], and the addition of Sc strongly improves the microstructures of aluminum alloys and their mechanical properties so that these aluminum alloys are suitable for use in aerospace and aeronautic applications [7–9]. Consequently, Sc determination in aerospace aluminum alloy is important to ensure the quality and guarantee the mechanical and chemical properties for aeronautic applications.

Inductively coupled plasma optical emission spectrometry (ICP-OES) has been demonstrated to be a powerful technique for determining chemical elements because of its high sensitivity and simultaneous determination capability [10]. Despite the use of ICP-OES for Sc determination in various types of samples (mainly geological materials) [11, 12] and elemental determination in aluminum alloys [13, 14], the use of ICP-OES for Sc determination in aluminum alloys is infrequently reported in the literature. Sc determination in aluminum alloys presents some challenges related to the complex matrix composition and relatively low amount of Sc (~0.1–0.2%) in these alloys [15]. The main constituents of aluminum alloys are aluminum, zinc, magnesium, and copper. These elements cause high levels of chemical or spectral interference due to the matrix complexity [16]. In particular, the aluminum matrix effect strongly interferes in the determination of chemical elements when ICP-OES is used as an analytical technique [17]. It has been reported that the matrix effect depends on the operational conditions of ICP-OES, and this matrix effect can be reduced under certain conditions [18]. Therefore, an in-depth study to establish the optimum operational conditions of ICP-OES for Sc determination is crucial for obtaining reliable results with a high level of sensitivity, great precision and accuracy, and the lowest limit of detection. A procedure to optimize the operational conditions to improve the sensitivity and signal-to-background ratio (SBR) is thus sought. Typically, the instrument operational conditions of ICP-OES are optimized using univariate optimization or orthogonal experiments, but these optimization designs suffer from prominent drawbacks, high consumption of time and financial resources, and the impossibility of evaluating interaction between the studied variables.

Recently, multivariate optimization techniques that allow optimization of analytical methods with higher efficiency than univariate and orthogonal optimization have been gaining ground in analytical chemistry [19–22]. Among the most relevant multivariate optimization techniques used in analytical optimization is response surface methodology (RSM), such as the factorial design, central composite design, Doehlert design, and Box–Behnken design. This methodology can be well applied when a response of interest is influenced by several variables. The objective is to simultaneously optimize the levels of these variables to attain the best system performance [23].

According to the literature, most of the studies on the application of RSM in the establishment of optimal instrument parameters of ICP-OES relate to the factorial design, central composite design, and Doehlert design. M. de O. Souza et al. used a 2^3 factorial design and a central composite design to optimize the nebulizer gas flow rate, auxiliary gas flow rate, and radio frequency power to evaluate the best operational conditions of ICP-OES [24]. A central composite design was used by G. Vanini et al. to evaluate the radio frequency, nebulizer gas flow rate, and aspiration rate [25]. The use of the Doehlert design to optimize the operational conditions of ICP for the determination of La, Nd, Eu, Gd, Dy, Er, and Yb was proposed by A. K. Guimaraes-Silva et al., who studied four factors: radio frequency, nebulizer gas flow rate, sample uptake rate, and observation height [16]. However, in contrast, the application of the Box–Behnken design, which allows the efficient estimation of the first- and second-order coefficients of the mathematical model to optimize ICP-OES operational conditions, is limited. Fernanda A. de Santana et al. proposed a direct method for the determination of gallium in bauxite samples by ICP-OES, and the experimental parameters were optimized by the Box–Behnken design [17]. A procedure was developed by C. G. Novaes et al. for optimization of the instrumental conditions of ICP-OES spectrometer using a two-level full factorial design, followed by the Box–Behnken design [26]. However, papers that utilize the Box–Behnken design to investigate the optimization of ICP-OES operational conditions for rare earth element determination are still lacking.

In the present study, the Box–Behnken design was employed to optimize the operational conditions for determining Sc in aluminum alloy samples by ICP-OES. The optimum analytical conditions obtained were used to determine the figures of merit of the method and to quantify Sc in aerospace aluminum alloys.

Experimental. Instrumentation. Measurements were performed using an inductively coupled plasma optical emission spectrometer (Perkin Elmer, Model Optima 7000 DV, USA) with an axial plasma configuration. The analytical line was selected for investigation: Sc, 361.383 nm. A digital display electric heating plate (LabTech Co. Ltd., Beijing, China) was used for sample decomposition.

Reagents, solutions, and samples. Reagents of analytical grade were used: 35% hydrochloric acid and 70% nitric acid (Fengchuan Chemical Reagent Technology Co. Ltd., Tianjin, China). Ultra-pure water (resistivity ≥ 18.2 M Ω /cm) was prepared with an ultra-pure water purification system (ROUP Technology Co. Ltd., Tianjin, China). A high-purity single-element stock standard solution of Sc (1 mg/mL, National Center of Analysis and Testing for Nonferrous Metals and Electronic Materials, Beijing, China) was employed for the preparation of calibration curves. All glassware employed for the ICP-OES analyses was stored overnight in a 10% nitric acid solution bath for cleaning. The glassware was rinsed with ultra-pure water before use and dried in a dust-free environment. Three aluminum alloy certified reference materials (CRMs) were used to evaluate the accuracy in the proposed operating conditions: GBW02220, GBW02222, and E5103 purchased from the National Research Centre (NCS Testing Technology Co. Ltd., Beijing, China).

Sample preparation. Portions of 0.1000 g of each sample were accurately weighed in a 50 mL beaker, and a mixture of 3 mL of concentrated HNO₃, 2 mL of concentrated HCl and 5 mL ultra-pure water was added to the same container by slowly pouring it into the sample, followed by heating to 120°C. After complete decomposition of the sample, the heating was ceased, and the solution was naturally cooled to room temperature. Then the solution was completely transferred to a 100 mL calibrated flask and diluted to the desired volume with ultra-pure water to produce the sample solution. This decomposition process was performed for each sample in all cases in quintuplicate.

Optimization procedure. First, optimization was performed using the Box–Behnken design, considering three variables: radio frequency (RF) power, nebulizer gas flow rate, and sample flow rate. All optimization experiments were performed using a Sc standard solution of 1 mg/L in random order, and quintuplicates of the center point were obtained to evaluate the experimental error. The analytical responses were recorded as SBR, which can be calculated using the equation $SBR = (I_{Analyte} - I_{Blank})/I_{Blank}$. The experimental data were then processed using Design Expert 8.0 software (Stat-Ease Inc., Minneapolis, MN, USA) to determine the optimum value of these variables. The variables and levels used in the Box–Behnken design are described in Table 1.

TABLE 1. Factors and Levels Used in the Box-Behnken Design for Optimization of ICP-OES Operating Conditions

No.	Variable	Low level	Central point	High level
		–1	0	1
A	RF power, W	900	1100	1300
B	Nebulizer gas flow rate, L/min	0.6	0.8	1.0
C	Sample flow rate, mL/min	0.9	1.2	1.5

Method validation. The calibration curves were established under the optimum conditions and three sets of poor conditions. The background equivalent concentration (BEC) and limits of detection and quantification (LOD and LOQ, respectively) were calculated according to IUPAC recommendations. The slope of each of the curves, BEC, LOD, and LOQ, under the optimum conditions and three sets of poor conditions were compared to verify the optimization validity.

The accuracy of the analytical method employing the optimum condition was evaluated following recommendations of the Eurachem/CITAC guide [27], in which the absolute difference (Δm) between the mean measured value (C_m) and the certified value (C_{CRM}) is calculated as $\Delta m = |C_m - C_{CRM}|$ and the uncertainty of Δm is $u\Delta$, which is calculated from the uncertainty of the certified value (u_{CRM}) and the uncertainty of the measurement result (u_m) according to the following equation: $u\Delta = \sqrt{u_m^2 + u_{CRM}^2}$, where u_m is obtained by dividing the expanded uncertainty of the measurement result by the square root of the number of measurements, and u_{CRM} is obtained by dividing the stated expanded uncertainty of the certified value by the cove-

rage factor or the t -factor for a 95% confidence level with $n-1$ degrees of freedom, n being the number of laboratories. The expanded uncertainty $U\Delta$, corresponding to a confidence level of approximately 95%, is obtained according to the equation: $U\Delta = 2u\Delta$. To evaluate the method performance, Δm is compared with $U\Delta$: if $\Delta m \leq U\Delta$, then there is no significant difference between the measurement result and the certified value.

Moreover, the accuracy of the method was evaluated by recovery studies of spiked samples. The certified reference materials GBW02220 and GBW02222 were spiked with variable quantities of Sc (between 0.2 and 5.0 mg/L). Recovery was calculated by the difference between analytical results obtained for spiked and un-spiked solutions, expressed as a percentage.

Results and discussion. *Optimization of instrumental variables for Sc determination.* In the development of methods based on ICP-OES, various instrumental variables, such as the RF power, sample flow rate, auxiliary gas flow rate, nebulizer gas flow rate, and refrigeration gas flow rate, can be adjusted to obtain a plasma with good performance in the element determination. Among these variables, the RF power, sample flow rate, and nebulizer gas flow rate are considered the main variables regarding plasma [28, 29]; so the RF power, nebulizer gas flow rate, and sample flow rate were simultaneously optimized using the data obtained from 17 sets of experiments carried out according to the Box–Behnken design. Generally, the instrument variable response was recorded as emission intensity in the optimization of ICP-OES operating conditions [17, 30]. However, it is noticeable that the instrumental variables also have a direct influence on background intensity for ICP-OES. It can be seen in Fig. 1a that there was an increase in the analyte intensity of Sc (I_{Analyte}) when increasing RF power, while an increase in power also increased the background intensity (I_{Blank}). Figure 1b shows that the analyte intensity of Sc (I_{Analyte}) first increases and then decreases with increasing nebulizer gas flow rate, while the background intensity (I_{Blank}) decreases with increasing nebulizer gas flow rate. In this way, SBR should be the response function of the Box–Behnken design model in order to optimize ICP-OES operational conditions since it is correlated with the limit of detection.

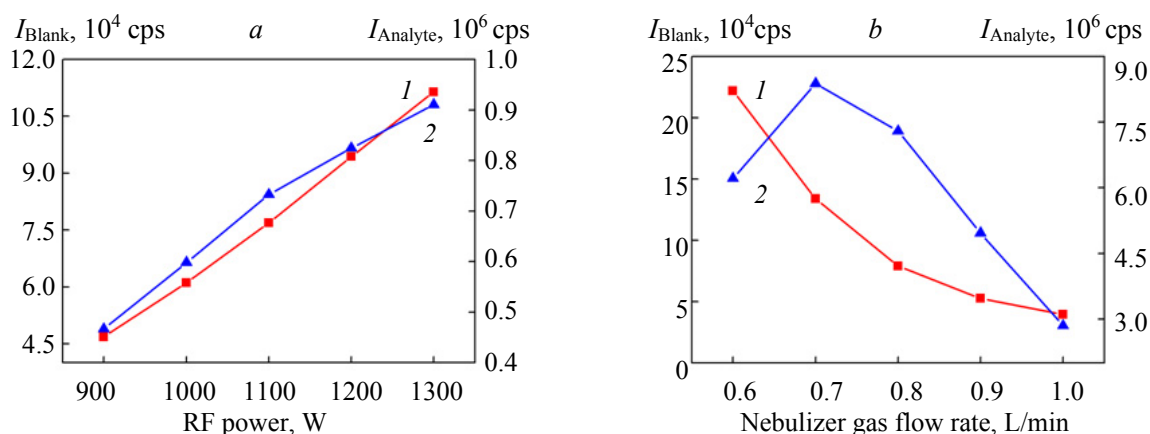


Fig. 1. Influence of RF power (a) and nebulizer gas flow rate (b) on I_{Blank} and I_{Analyte} of Sc, background (1) and analyte (2) intensity.

In this paper, SBR for Sc was investigated as the response function of the Box–Behnken design model in order to optimize ICP-OES operational conditions. The levels of the operating variables, analyte intensity (I_{Analyte}), background intensity (I_{Blank}), and the response value are presented in Table 2.

The experiment runs were randomized in order to minimize the effect of uncontrolled factors [31]. The analysis of variance (ANOVA) was used to evaluate the significance of the model equation and related terms. The experimental relationship between SBR for Sc and the three factors in coded units obtained by the application of response surface methodology was expressed in terms of the following equation:

$$Y = 30.32 + 0.75A + 0.23B - 0.55C + 4.82AB - 0.23AC + 1.02BC - 0.97A^2 - 13.27B^2 - 0.52C^2,$$

where A , B , and C correspond to independent variables of RF power, nebulizer gas flow rate, and sample flow, respectively, while the terms AB , BC , and AC correspond to the interactions of the variables. The overall ANOVA results demonstrated that the models and interaction terms of AB and B square were significant at the 95% confidence level, which indicated that the nebulizer gas flow rate and the interaction of nebulizer gas flow rate with RF power were the most critical parameters affecting plasma conditions.

TABLE 2. Lists of Experiments in the Box-Behnken Design

No.	A	B	C	$I_{Analyte}$	I_{Blank}	SBR	No.	A	B	C	$I_{Analyte}$	I_{Blank}	SBR
1	-1	0	1	2579156	86641	28.8	10	-1	-1	0	3696485	178860	19.7
2	0	0	0	3793513	120503	30.5	11	1	0	1	4986135	169403	28.4
3	0	0	0	3794223	121810	30.1	12	0	-1	1	3763299	253294	13.9
4	-1	0	-1	2583735	86680	28.8	13	0	0	0	4061350	124437	31.6
5	0	-1	-1	4927175	264014	17.7	14	0	1	-1	1507478	83353	17.1
6	0	0	0	3804949	122819	30.0	15	1	-1	0	4823444	345625	13.0
7	0	0	0	3847650	126747	29.4	16	1	1	0	2507788	108594	22.1
8	1	0	-1	4953190	163592	29.3	17	0	1	1	1563732	85120	17.4
9	-1	1	0	645006	61710	9.5							

Figure 2 shows the three-dimensional response surface plot for SBR of Sc; it should be noted that the three-dimensional response surface plots were constructed as a function of two factors. The sample flow rate, which had a minor effect compared to that of the RF power and nebulizer gas flow rate, was maintained at a fixed level (central point 0.8 mL/min) in order to understand the main effect and interaction effect of the two factors (RF power and nebulizer gas flow rate). It can be seen from Fig. 2 that the results for SBR of Sc had a maximum point within the studied experimental domain. The solution of the above quadratic equation shows that the best SBR of Sc is obtained with an RF power of 1300 W, a nebulizer gas flow rate of 0.83 L/min, and a sample flow rate of 0.9 mL/min.

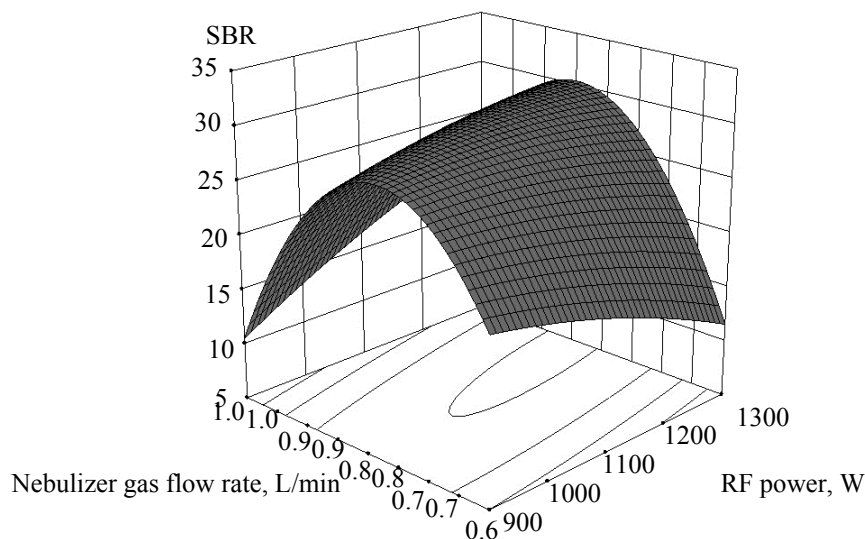


Fig. 2. Responses surface created by Box-Behnken design in the optimization of Sc determination.

Analytical features. The calibration curves were prepared with seven points for the concentrations of Sc 0, 0.1, 0.3, 1.0, 5.0, 8.0, and 10.0 mg/L. To verify the optimization validity, four calibration curves were established under the optimum conditions and three sets of poor conditions (corresponding to the 9th, 12th, and 15th rows of Table 2).

Based on the resulting calibration curves, the performance characteristics were calculated. The slope of the calibration curves and all the other analytical parameters under the optimum conditions and the three sets of poor conditions are shown in Table 3. In this table, it can be seen that the method employing the optimum conditions (an RF power of 1300 W, a nebulizer gas flow rate of 0.83 L/min, and sample flow rate of 0.9 mL/min) was the most sensible and had the lowest BEC, LOD, and LOQ, and these values indicate that a reliable result with a high level of sensitivity and the lowest limit of detection can be achieved employing the optimum conditions.

TABLE 3. Comparison of Performance Characteristics under the Optimum Conditions and Poor Conditions

No.	RF power, W	Nebulizer gas flow rate, L/min	Sample flow rate, mL/min	Slope	BEC, $\mu\text{g/L}$	LOD, $\mu\text{g/L}$	LOQ, $\mu\text{g/L}$
1	1300	0.83	0.9	63090000	11.5	0.15	0.48
2	900	1.0	1.2	7308000	17.9	0.24	0.79
3	1100	0.6	1.5	35200000	47.1	0.66	2.21
4	1300	0.6	1.2	40030000	59.4	0.98	3.25

Validation of the proposed method. The accuracy of the analytical method employing the optimum conditions was evaluated by analysis of certified reference material E5103. The results are shown in Table 4, where C_{CRM} is the certified value and C_m is the mean measured concentration, u_{CRM} is the uncertainty of the certified value, and u_m is the uncertainty of the measurement result. As seen, the absolute difference (Δm) between the mean measured value (C_m) and the certified value (C_{CRM}) was lower than the expanded uncertainty U_Δ , so there was no significant difference between the certified value and the concentration obtained by the proposed method.

TABLE 4. Analytic Results (wt%) for Sc in Certified Reference Material E5103 ($n = 10$)

Reference material	C_{CRM}	u_{CRM}	C_m	u_m	Δm	U_Δ	RSD
E5103	0.181	0.0012	0.179	0.0013	0.002	0.0035	0.63

The accuracy of the method was further verified in the recovery study. The results obtained are presented in Table 5. As can be observed, recoveries varied from 96.5 to 105.0%. Table 5 also includes the precision of results, expressed as relative standard deviation (RSD). As observed, for concentrations of Sc in the range of 0.020–0.500%, the precision was 0.58–2.30%, which indicated the possibility of continuous analysis of samples with adequate accuracy.

TABLE 5. Recovery Study of Sc Concentrations in Spiked Aluminum Alloy Samples ($n = 10$)

Sample	Added value, %	Achieved value $\pm U_a$, %	Recovery, %	RSD, %
GBW02222	0.020	0.021 \pm 0.002	105.0	2.3
	0.050	0.049 \pm 0.002	98.0	1.2
	0.100	0.100 \pm 0.004	100.0	0.95
	0.200	0.193 \pm 0.003	96.5	0.84
GBW02220	0.350	0.338 \pm 0.004	96.6	0.58
	0.500	0.487 \pm 0.006	97.4	0.91

Note. U_a is the expanded uncertainty for the 95% confidence level;
Recovery = (Achieved value – Added value) / Added value \times 100.

TABLE 6. Analytic Results for Sc Concentrations in Real Aluminum Alloy Samples ($n = 10$)

No.	Achieved value $\pm U_a$, %	Added value, %	Total value $\pm U_a$, %	Recovery, %
1#	0.139 \pm 0.002	0.140	0.277 \pm 0.004	98.6
2#	0.171 \pm 0.002	0.150	0.318 \pm 0.004	98.0
3#	0.196 \pm 0.003	0.200	0.395 \pm 0.005	99.5
4#	0.251 \pm 0.003	0.200	0.452 \pm 0.005	100.5

Note. U_a is the expanded uncertainty for the 95% confidence level;
Recovery = (Total value – Achieved value) / Added value \times 100.

Analysis of real samples. To assess the applicability of the proposed method to real samples, the proposed method was applied to the Sc determination in real aluminum alloy samples from the Beijing Institute of Aeronautical Materials. The results obtained are presented in Table 6. Moreover, the accuracy of the results was confirmed by performing a standard addition method. As can be seen, recoveries varied from 98.0 to 100.5%.

Conclusions. The response surface method allowed us to obtain the optimum operational conditions for Sc determination in aluminum alloy samples by ICP–OES (RF power: 1300 W, nebulizer gas flow rate 0.83 L/min, and sample flow rate: 0.9 mL/min). The large interaction effect of RF power and nebulizer gas flow rate on the SBR of Sc during Sc determination by ICP–OES was demonstrated. The proposed method showed that there was no significant difference between the measured value and the certified value. The RSD values of the proposed method were less than or equal to 2.0%, and the method showed a relatively low LOD (0.15 µg/L) and LOQ (0.48 µg/L). The method developed was applied to the determination of scandium in aluminum alloys, and the recovery study results ranged between 98.0 and 100.5%.

Acknowledgments. The author would like to acknowledge the Research Institute of Physical and Chemical Engineering of Nuclear Industry for support of this research.

REFERENCES

1. F. Sun, G. L. Nash, Q. Li, E. Liu, C. He, C. Shi, N. Zhao, *J. Mater. Sci. Technol.*, **33**, 1015–1022 (2017).
2. S. Zivkovic, J. Savovic, M. Trtica, J. Mutic, M. Momcilovic, *J. Alloys Compd.*, **700**, 175–184 (2017).
3. G. Li, N. Q. Zhao, T. Liu, J. J. Li, C. N. He, C. S. Shi, E. Z. Liu, J. W. Sha, *Mater. Sci. Eng. A*, **617**, 219–227 (2014).
4. V. Senkova, O. N. Senkov, D. B. Miracle, *Met. Mater. Trans. A Phys. Met. Mater. Sci.*, **37**, 3569–3575 (2006).
5. M. Zhang, T. Liu, C. He, J. Ding, E. Liu, C. Shi, J. Li, Naiqin, *J. Alloys Compd.*, **658**, 946–951 (2016).
6. H.-R. Stock, B. Köhler, H. Bomas, H.-W. Zoch, *Mater. Des.*, **31**, S76–S81 (2010).
7. R. E. S. Froes, W. B. Neto, R. L. P. Naveira, N. C. Silva, C. C. Nascentes, J. B. B. da Silva, *Microchem. J.*, **92**, 68–72 (2009).
8. T. Grigoletto, E. de Oliveira, I. G. R. Gutz, *Talanta*, **67**, 791–797 (2005).
9. A. Muhammad, C. Xu, W. Xuejiao, S. Hanada, H. Yamagata, L. Hao, M. Chaoli, *Mater. Sci. A: Struct. Mater.*, **604**, 122–126 (2014).
10. M. de O. Souza, M. A. Ribeiro, M. T. W. D. Carneiro, G. P. B. Athaude, E. V. R. de Castro, F. L. E. da Silva, W. O. Matos, *Fuel*, **154**, 181–187 (2015).
11. K. Satyanarayana, S. Durani, G. V. Ramanaiyah, *Anal. Chim. Acta*, **376**, 273–281 (1998).
12. J. Połedniok, *Chemosphere*, **73**, 572–579 (2008).
13. N. Carrion, A. M. Itriago, M. A. Alvarez, E. Eljuri, *Talanta*, **61**, 621–632 (2003).
14. T. Grigoletto, E. de Oliveira, I. G. R. Gutz, *Talanta*, **67**, 791–797 (2005).
15. Y. Shi, Q. Pan, M. Li, X. Huang, B. Li, *Mater. Sci. A: Struct. Mater.*, **621**, 173–181 (2015).
16. A. K. G. Silva, J. C. de Lena, R. E. S. Froes, L. M. Costa, C. C. Nascentes, *J. Braz. Chem. Soc.*, **23**, 753–762 (2012).
17. F. A. de Santana, J. T. P. Barbosa, G. D. Matos, M. G. A. Korn, S. L. C. Ferreira, *Microchem. J.*, **110**, 198–201 (2013).
18. M. T. Larrea, B. Zaldivar, J. C. Farinas, L. G. Firgaira, M. Pomares, *J. Anal. At. Spectrom.*, **23**, 145–151 (2008).
19. C. G. Novaes, M. A. Bezerra, E. G. P. de Silva, A. M. P. Santos, I. L. S. da Romao, J. H. S. Neto, *Microchem. J.*, **128**, 331–346 (2016).
20. R. F. de Oliveira, C. C. Windmoller, W. B. Neto, C. C. Souza, M. A. Beininger, J. B. B. Silva, *Anal. Method.*, **5**, 5746–5752 (2013).
21. N. M. L. Araujo, S. L. C. Ferreira, H. C. Santos, D. S. Jesus, M. A. Bezerra, *Anal. Methods*, **4**, 508–512 (2012).
22. M. Khajeh, *J. Hazard Mater.*, **172**, 385–389 (2009).
23. M. A. Bezerra, R. E. Santelli, E. P. Oliveira, L. S. Villar, L. A. Escaleira, *Talanta*, **76**, 965–977 (2008).
24. M. de O. Souza, K. P. Rainha, E. V. R. Castro, M. T. W. D. Carneiro, R. D. Q. Ferreira, *Quim. Nova*, **38**, 980–986 (2015).

-
25. G. Vanini, M. O. Souza, M. T. W. D. Carneiro, P. R. Filgueiras, R. E. Bruns, W. Romao, *Microchem. J.*, **120**, 58–63 (2015).
 26. C. G. Novaes, S. L. C. Ferreira, J. H. S. Neto, F. A. de Santana, L. A. Portugal, H. C. Goicoechea, *Curr. Anal. Chem.*, **12**, 1–8 (2016).
 27. S. L. R. Ellison, A. Williams. *Comparison of a Measurement Result with the Certified Value*. Eurachem/CITAC Guide, ISBN 978-0-948926-30-3 (2012).
 28. R. E. S. Froes, W. B. Neto, N. O. C. Silva, R. L. P. Naveira, C. C. Nascentes, J. B. B. da Silva, *Spectrochim. Acta, B: At. Spectrosc.*, **64**, 619–622 (2009).
 29. J. C. Farinas, I. Rucandio, M. S. P. Alfonso, M. E. V. Tagle, M. T. Larrea, *Talanta*, **154**, 53–62 (2016).
 30. J. S. Santos, L. S. G. Teixeira, R. G. O. Araujo, A. P. Fernandes, M. G. A. Korn, S. L. C. Ferreira, *Microchem. J.*, **97**, 113–117 (2011).
 31. P. N. Nomngongo, J. C. Ngila, T. A. M. Msagati, B. Moodley, *Microchem. J.*, **114**, 141–147 (2014).